Bioresource Technology 244 (2017) 198–205

Contents lists available at ScienceDirect

Bioresource Technology

journal homepage: www.elsevier.com/locate/biortech

Impact of the accumulation and adhesion of released oxygen during *Scenedesmus obliquus* photosynthesis on biofilm formation and growth

Yaping Zheng, Yun Huang*, Qiang Liao, Qian Fu, Ao Xia, Xun Zhu

Key Laboratory of Low-grade Energy Utilization Technologies and Systems, Chongqing University, Ministry of Education, Chongqing 400044, China
Institute of Engineering Thermophysics, Chongqing University, Chongqing 400044, China

GRAPHICAL ABSTRACT

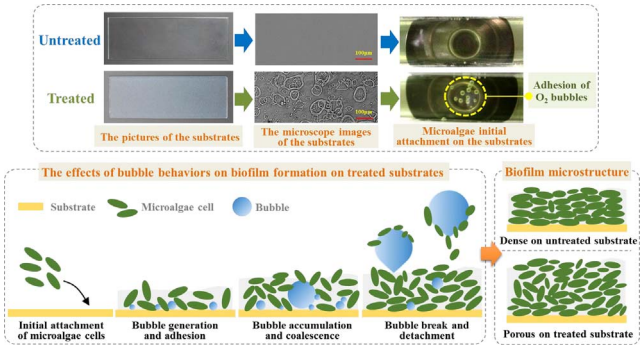

ARTICLE INFO

Keywords:
Microalgae biofilm
PTFE emulsion
Surface wettability
Bubble adhesion
Porosity

ABSTRACT

Microalgae cells release O_2 during photosynthesis. The gas can accumulate and adhere in form of bubbles, which affect the transport of nutrients in the biofilm and the biofilm microstructure. To investigate the reasons for the adhesion of these oxygen bubbles and their impact on biofilm, polytetrafluoroethylene (PTFE) emulsion was sprayed onto glass surface to change the parameters for gas accumulation and adhesion. The results indicated gas could aggregate into bubbles and adhere to hydrophobic and rough surface. The bubble behaviors caused the biofilm to be porous (with a microporosity of 9.43–20.94%). The biomass concentration of the more porous biofilm increased by 9.26% to 22.42 g m^{-2} on 1% PTFE-treated surface compared to that on an untreated surface. However, with an increase in PTFE concentration, the amount of adhered bubbles increased. More microalgae cells in biofilms were carried up by bubbles. The biofilm concentration on 5% PTFE-treated surface decreased by 15.30%.

1. Introduction

Due to the scarcity of energy and the environmental pollution resulting from the use of fossil fuels, the exploration of alternative, renewable and clean energy sources has become a critical issue (Yang et al., 2017). As a third-generation biomass energy source, microalgae have attracted much focus during the past several decades due to their superiority in the producing large biomass amounts and fixing large amounts of CO_2 efficiently (Chang et al., 2017; Shen et al., 2016; Sun et al., 2016).

Traditional cultivation, i.e., a suspended system, has been shown to be expensive for cell harvesting due to the high water content needed for the microalgae suspension (99.5%) (Tsolcha et al., 2015). Thus, there is a great interest in the development of a new cultivation type by

* Corresponding author at: Key Laboratory of Low-grade Energy Utilization Technologies and Systems, Chongqing University, Ministry of Education, Chongqing 400044, China.
E-mail address: yunhuang@cqu.edu.cn (Y. Huang).

http://dx.doi.org/10.1016/j.biortech.2017.07.145
Received 24 May 2017; Received in revised form 22 July 2017; Accepted 24 July 2017
Available online 27 July 2017
0960-8524/

using biofilms, because microalgae cultivated in such systems have a lower water requirement and a very high biomass density (8–16% g/g) (Christenson & Sims, 2012; Schnurr et al., 2014) compared to cultivated in suspended systems (-0.6% g/g) (Chang et al., 2016; Chisti, 2007). The high biomass concentration of biofilms makes it easy to harvest the microalgae (Gross et al., 2015; Shen et al., 2009; Stephens et al., 2010). A previous study confirmed that *Chlorella vulgaris* produced 30.4% higher biomass levels (103 g m^{-2}) in a biofilm system than in a suspended system (Huang et al., 2016). Biomass that is very highly concentrated can be scraped off the supporting material surface and directly used to produce biofuel without costly harvesting techniques such as centrifugation or filtration (Berner et al., 2015). Therefore, the energy requirement to harvest the biomass was reduced by 99.7% compared to harvesting biomass from a microalgae suspension in previous research (Ozkan et al., 2012).

As for the biofilm cultivation, microalgae cells attach on the substrate under the effect of electrostatic force, Van der Waals force, surface tension, etc., then develop to stable biofilm through continued growth (Wang & Wei, 2009). Therefore, biofilm formation and growth are greatly affected by the properties of the substrate, including wettability, roughness, texture, and charge property, among others (Schnurr & Allen, 2015). During the processes of biofilm formation and growth, microalgae undergo photosynthesis, synthesize organic matter, store energy and release oxygen gas. Previous research has indicated that the oxygen gas released by microalgae photosynthesis could adhere to the PTFE-treated surface in the form of bubbles (Zheng et al., 2016). However, bubble behaviors always cause microalgae cells to distribute non-uniformly under the action of bubble carrying (Huang et al., 2017). Liu et al. (Liu et al., 2014) found that biofouling biofilm on the membrane became more porous after the cleaning process in a microbubble-aerated reactor. In addition, Gião et al. (2005) verified that bubbles may contribute to the detachment of adhering cells or the biofilm growth on the electrode surface. Alternatively, in some cases, bubbles around the cells impede the transfer and exchange of nutrients between the cells and the medium (Liao et al., 2007; Qu et al., 2011). Thus, it can be concluded that adhered bubbles formed by O_2 released from microalgae cells play an important role during the processes of biofilm formation and growth. Additionally, the behavior of these bubbles may impact the biofilm microstructure, biofilm thickness, biomass accumulation, and other factors. Zheng et al. (2016) confirmed that biofilm biomass on a treated surface (with adhesion bubbles) increased by 16.86% compared to that on an untreated surface (without adhered bubbles). This new phenomenon indicated that adhered bubbles could optimize the formation and growth of biofilm under certain conditions. Nevertheless, few published studies have been focused on the effects of bubble behavior on microalgae biofilm formation and growth. There is also a scarcity of research describing the reasons for the emergence and adhesion of bubbles around the microalgae biofilm on some material surfaces. Due to the lack of relevant research, the optimized conditions for biofilm formation and growth cannot be determined on the basis of reliable research conclusions at this time.

Therefore, the substrate surfaces that the biofilm attaches to were treated with varying concentration of a PTFE emulsion in this study. The surface properties were tested to clarify the reasons for bubble adhesion. The bubble behaviors on the substrates and their effects on biofilm formation and growth were also investigated at both the initial attachment phase and the sustained growth phase of the biofilm development.

2. Materials and methods

2.1. Microalgae strains and culture

Scenedesmus obliquus strain FACHB-417 was purchased from the Institute of Hydrobiology, Chinese Academy of Sciences (Wuhan, China). The stock culture was maintained in Blue-Green medium (BG11) consisting of 750 mg L^{-1} $NaNO_3$, 40 mg L^{-1} K_2HPO_4, 75 mg L^{-1} $MgSO_4{\cdot}7H_2O$, 36 mg L^{-1} $CaCl_2{\cdot}2H_2O$, 6 mg L^{-1} citric acid, 6 mg L^{-1} ferric ammonium citrate, 1 mg L^{-1} EDTA-Na, 20 mg L^{-1} Na_2CO_3, 2.86 mg L^{-1} H_3BO_3, 1.86 mg L^{-1} $MnCl_2{\cdot}4H_2O$, 0.22 mg L^{-1} $ZnSO_4{\cdot}4H_2O$, 0.39 mg L^{-1} $Na_2MoO_4{\cdot}2H_2O$, 0.08 mg L^{-1} of $CuSO_4{\cdot}5H_2O$ and 0.05 mg L^{-1} of $Co(NO_3)_2{\cdot}6H_2O$. The pH of the medium was adjusted to 7.0 with 0.1 M HCl, and the medium was autoclaved before use. The batch was cultivated at 25 °C under a light intensity of 90 μmol m^{-2} s^{-1}.

2.2. Substrate surface treatment and characterization

For easy of tests and analysis, the glass slides (25.4 × 76.2 × 1 mm) were applied in this study. All the substrates (glass slides) used in the experiments were thoroughly washed with alcohol before use. For the surface treatment of the glass slides, varying concentrations of a polytetrafluoroethylene (PTFE) emulsion (HESEN, Shanghai) were uniformly sprayed onto the glass slides. Then, the glass slides were sintered in a drying oven at 350 °C and left for 30 min. Subsequently, the substrates cooled naturally and were used for the following measurements and experiments.

2.2.1. Wettability measurement

Wettability can be represented by the contact angle between drops of liquid resting on a solid substrate. The sessile drop experiment (Bachmann et al., 2000) was generally recognized as the common method to determine the contact angle in many studies. The tests were repeated at five random loci of each substrate, and the surface wettability of each substrate was represented by the average value of the contact angles. The reproducibility in the contact angle tests was approximately ± 2°. To avoid operator error, the qualified substrates were chosen as the experimental substrates based on the results of these contact angle tests.

2.2.2. Roughness and morphology measurement

The surface roughness and morphology were measured by a surface profilometer (Veeco Dektak 150, American). The stylus radius, the contact force and the measurement length were set at 2.5 μm, 3 mg and 4000 μm, respectively. The roughness value was the average number of the value at three random loci for each tested coupon.

2.3. Experimental setup

The experiment was conducted in the following two stages. One stage examined the initial formation of the *S. obliquus* biofilm, while the other stage examined the growth of *S. obliquus* on the biofilm.

For the first stage, photobioreactor (50 × 10 × 10 mm) with different bottom surfaces was placed on the objective table of the microscope (IX81, Olympus). In order to inspect and calculate easily and accurately, only one milliliter of the microalgae suspension ($OD_{680\ nm}$ = 1.0) was inoculated into every photobioreactor (PBR). Additionally, the light intensity was very low, about 5 μmol m^{-2} s^{-1}, to avoid being influenced by microalgae growth. The microscope was used to record changes in the biofilm and bubbles at set intervals. Then, microalgae cell numbers were counted through the microscope images.

In the second stage, each substrate (76.2 × 25.4 × 1 mm) was immobilized on the bottom of a polymethyl methacrylate PBR (80 × 30 × 45 mm). The initial inoculum of the suspended microalgae was 45 mL ($OD_{680\ nm}$ = 1.5) for every PBR. Then, all of the PBRs were statically cultured in an artificial conservatory where the temperature was controlled at 26 ± 1 °C, the light intensity was 90 μmol m^{-2} s^{-1} and the carbon dioxide was captured from the surrounding air.

2.4. Analysis methods of biofilm characteristics

Two parallel samples were sampled every 24 h. The sampling

processes were described as follows. First, the supernatant in the PBR was removed. Then, the biofilm on the substrate was washed with sterile distilled water and diluted to 25 mL in a volumetric flask. The resuspension was subsequently prepared for further measurement and analysis.

2.4.1. Biomass and chlorophyll concentration

During cultivation, the microalgae biomass concentration was determined by measuring the optical density of a microalgae suspension at an absorbance of 680 nm (OD_{680}) using a UV–Visible spectrophotometer (Persee TU-1901, China) every 24 h. The samples were diluted to ensure OD_{680} values within 0.1 ~ 1.0 to accurately correlate the optical density with the microalgae biomass concentration. The relationship between the OD_{680} and the dry biomass concentration of *S. obliquus* was established according to Eq. (1):

$$D_w = 2.6634 \times OD_{680} + 0.1318 \quad (R^2 = 0.99) \tag{1}$$

where D_w is the microalgae biomass concentration (g m^{-2}).

Chlorophyll was extracted with a mixture of dimethyl sulfoxide (DMSO)/80% and acetone (1/2, V/V) and then measured according to the method of Lorenzen (Lorenzen, 1967).

2.4.2. Biofilm thickness and porosity

The substrate covered with biofilm was removed from the PBRs and gently rinsed with sterile water to remove any unattached cells. Following this pre-preparation, the biofilm coupons were fixed, stained and dehydrated in the proper sequence as described by Surman et al. (1996). The coupons then remained desiccated and were gold sputtered using a sputter coater and viewed in a scanning electron microscopy (SEM) (TESCAN, VEGA3). The biofilm thickness data were obtained from the SEM imaging processing software, Digimizer. From the SEM images of biofilm sections, the porosities of biofilm sections were calculated with the digital image processing program Adobe Photoshop (Tang et al., 2010; Zhang et al., 2014). The pore areas (A_p) and the total section areas (A_t) were obtained. Then, the porosity (P) was calculated using the following equation:

$$P = A_p/A_t \times 100\% \tag{2}$$

2.4.3. Image acquisition and analysis of adhered bubbles

The dynamic changes of the bubbles were recorded regularly using a Nikon D80 camera with a macro lens. Following the scale plates pasted at the bottom of the PBRs, the images were analyzed using the software, Digimizer. The changes of bubble area per unit length was calculated with the following Eq. (3):

$$Y = A_b/L \tag{3}$$

where Y is the bubble area per unit length (cm^2 cm^{-1}), A_b is the total bubble area (cm^2), and L is the bubble covered length (cm).

3. Results and discussion

3.1. Accumulation and adhesion of released oxygen during S. obliquus initial attachment and growth

3.1.1. The initial attachment of microalgae cells on PTFE-treated surfaces

The initial attachment of microalgae cells is shown in Fig. 1. The cells settled and adhered to the substrate surfaces under the action of various forces (electrostatic forces, Van der Waals forces, and surface tension, among others) that were mainly determined by substrate surface properties (Wang and Wei, 2009). The attachment rates of the microalgae cells increased with increasing concentrations of the PTFE emulsion during the first 10 min. Subsequently, the results showed an opposite tendency. The attachment rate on the untreated substrate was significant higher than that on the treated substrate, and the attachment rates decreased as the PTFE emulsion increased. More importantly, small bubbles began to appear on the PTFE-treated surfaces after several minutes, but they did not appear on the untreated surface. The bubble formation may result in oxygen released from microalgae cells during photosynthesis. In addition, the small bubbles grew bigger with time, and then, they detached and rose in the liquid medium. For the experiment, the amount of microalgae cells inoculated to the photobioreactors were the same. The amount of new grown cells could be ignored for the limited time and light intensity. However, it observed that some microalgae cells adhered on the surfaces of the detached bubbles and were carried back into the liquid after 10 min. This might be the reason why the amount of microalgae cells attached showed an opposite tendency after 10 min. Thus, the surface that facilitates the attachment of microalgae cells is not necessarily suitable for microalgae growth. Therefore, it is necessary to test surface properties treated with various concentrations of PTFE.

3.1.2. The properties of the different substrate surfaces

As shown in Table 1, the contact angle of PTFE-treated substrate surfaces increased with the increased concentration of the PTFE emulsion due to its super-hydrophobicity. Furthermore, the super-hydrophobicity of the PTFE emulsion may be a significant factor affecting the attachment rate of cells during the first 10 min, as shown in Fig. 1. PTFE is defined as a nonpolar molecule because of its highly symmetrical molecular structure (Pereira et al., 2015). Interactions between polar molecules and a nonpolar polymer were weaker than the interactions between polar polymers (Rios et al., 2007). Therefore, the interaction between water and the PTFE-treated surface is weaker than the interaction between water and untreated glass. There is a layer of hydration laver upon the hydrophilic material surface (Zheng et al., 2012). Due to the stronger chemical bond energy, the untreated surface could combine with the hydration laver tightly and stably. These two characters cause that the microalgae cells in the bottom layer need to overcome a higher energy barrier and break the hydration laver, unlike the cells attached on the surface of the substrate. Consequently, the attachment rate of the microalgae cells increased during the first 10 min with the increase in hydrophobicity (Fig. 1).

To quantitate the surface roughness on the substrate, two parameters, Ra and Rq, were used in this section, and the results are shown in Table 1. Ra is defined as the average of the absolute values of the height deviation on the biofilm surface, whereas Rq is the root-mean-square of the height deviation. In addition, Fig. 2 displays the visual appearance of the surface roughness. The surface of the untreated substrate appeared smoother than that of the treated substrates. However, the roughness of the three substrates was all rather small and on a nanoscale level. However, the size of *S. obliquus* is approximately 10–20 μm. Obviously, there are considerable differences between the magnitude of the substrate roughness and the cell size. Therefore, the effect of roughness on the initial attachment and growth of the microalgae was not considered to affect this substrate treatment method. However, its effects on bubble behaviors could not be ignored.

From the insets in Fig. 2, the morphology of the untreated substrate surface was smoother than the treated surfaces. The microstructure concavo-convex was observed on the treated substrate surface. The profile or morphology of the treated substrate surface tended to exhibit both a higher peak value and a larger peak number. Furthermore, this tendency increased with the increase of contact angle. Additionally, a previous study (Attard, 2003) stated that the super-hydrophobic surfaces always existed with nanobubbles. A rougher and more hydrophobic material surface was observed to have more nanobubbles (Ditscherlein et al., 2016). Thus, the properties of the treated substrate surfaces could provide the conditions for the extension of nanobubbles. These nanobubbles would then act as bubble cores for oxygen adhesion on the substrate surface. Moreover, the departure radius of the bubbles became larger as the hydrophobicity of the material surfaces increased (Byakova et al., 2003). In contrast, due to the absence of this peculiar surface property, metabolic gas on the untreated surfaces directly

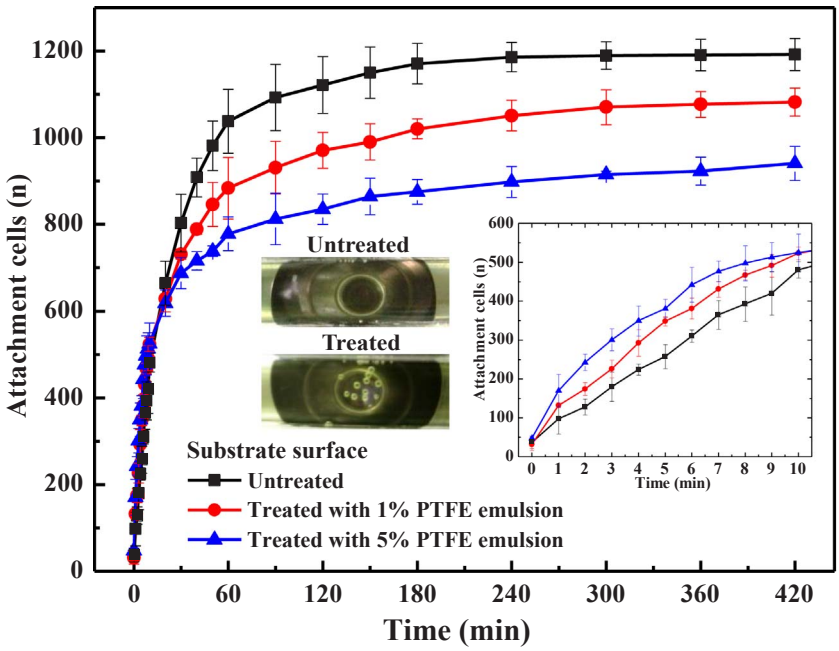

Fig. 1. The initial attachment of microalgae cells to different substrate surfaces.

Table 1
The surface properties of different substrate.

	Untreated	Treated with 1% PTFE emulsion	Treated with 5% PTFE emulsion
Contact angle	34°	64°	133°
Average roughness Ra/nm	2.49	105.52	176.21
Root-mean-square roughness Rq/nm	3.16	160.46	295.60

diffused and dissolved into the medium liquid and was no longer attached to the substrate surface.

3.1.3. Dynamic behaviors of adhesion bubbles on PTFE-treated surface

Fig. 3 is the changes of bubbles behaviors during the first 420 min at the initial attachment period. As observed from the insets in Fig. 3, the adhered bubbles first emerged around the sites that were in the light. These bubbles gradually grew and increased their growth rate after 40 min (Fig. 3), during which the microalgae cells had almost completely settled (Fig. 1). This phenomenon can be explained for that the microalgae at these sites conduct photosynthesis and release oxygen. Due to the substrate surface properties, oxygen adhered on the substrate in the form of bubbles. Bubble growth could contribute to the continuous gas released from the microalgae cells. With continued release of oxygen, the bubbles grew and began to coalesce into larger bubbles. Once the size of the coalesced bubbles became large enough, the bubbles broke, and part of the gas detached. The remaining smaller bubbles continued to grow.

During the initial attachment period, these adhered bubbles had a negative effect on biofilm formation. The attached bubbles occupied the growth space of the microalgae and the biofilm. Additionally, along with the bubble growth, break and departure, some microalgae cells in the biofilm would be carried into the medium liquid by bubbles due to the action of bubble carrying. Therefore, with the increase in the hydrophobicity, this adverse effect became more obvious. More bubbles would carry more microalgae cells away. The results in Fig. 1 also confirmed this conclusion.

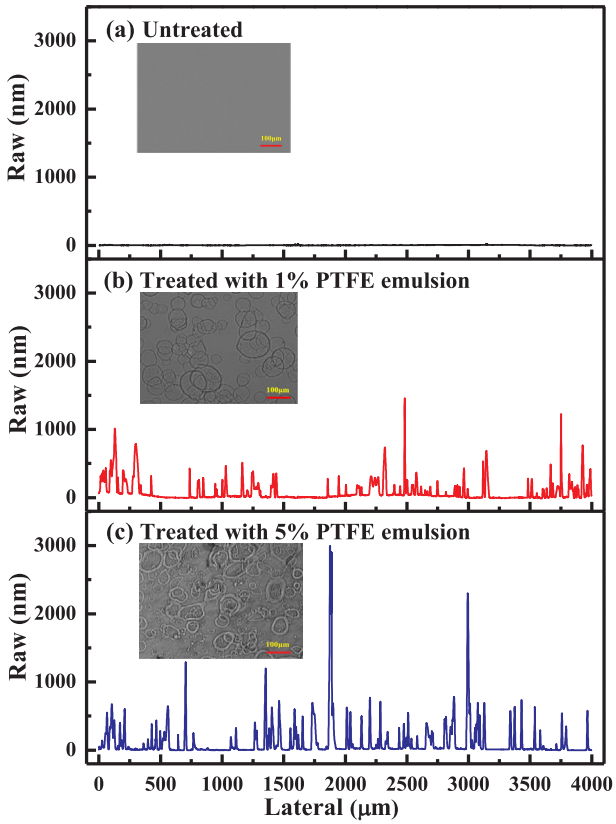

Fig. 2. The profiles of the substrate surfaces: (a) an untreated surface, (b) a surface treated with 1% PTFE emulsion and (c) a surface treated with 5% PTFE emulsion.

3.2. Effects of bubble behavior on S. obliquus biofilm formation and microstructure on PTFE-treated surfaces

Surface treatment could not only affect microalgae attachment but also play an important role in biofilm formation. Fig. 4 showed the changing curves of biomass concentration (Fig. 4a), biofilm thickness and porosity (Fig. 4b), bubble changing (Fig. 4d), and dissolved oxygen concentration (DO) (Fig. 4c) on substrate surfaces with a different

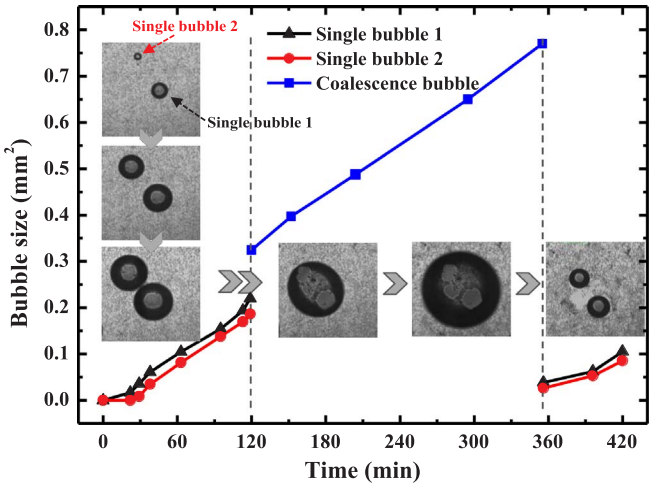

Fig. 3. The dynamic behaviors of adhered bubbles on substrate surface treated with 5% PTFE emulsion.

coating, respectively. As shown in Fig. 4a, a greater concentration of biofilm biomass accumulation occurred on the surface treated with 1% PTFE emulsion. The biomass yield obtained was 22.42 g m^{-2}, which was 9.26% higher than those on untreated substrates. Meanwhile, lower amounts of biomass accumulated on the surface treated with 5% PTFE emulsion. The biomass yield obtained was 17.28 g m^{-2}, which is 15.30% lower than those on untreated substrates. These results showed here were different from the results represented initial attachment period (Fig. 1). The possible reason was that there were only a small amount of microalgae cells adhered on the substrate surface. When the bubbles detached from the treated substrate surfaces, some cells would be carried away from the surfaces. Thus, there were more microalgae cells on untreated surfaces than that on treated surfaces at the later period of initial attachment. However, as for the long-term growth period, bubble carrying could contribute to the formation on a porous biofilm microstructure (Fig. 4b). Biofilm thickness on the 1% PTFE emulsion-treated surface reached 33.78 μm, which was thicker than the biofilm on the untreated substrate surface, which was 28.77 μm. Instead, the biofilm thickness on the 5% PTFE emulsion treated surface only reached 24.56 μm. It can be predicted that these differences may contribute to the diverse biofilm microstructure. The dotted lines in Fig. 4b present the biofilm porosity on different substrate surfaces. The biofilm porosities on the treated substrate surfaces were 9.43–20.94%; these porosities were much higher than those on the untreated substrate surfaces, which had porosities of 4.66–7.69%. In addition, the biofilm porosity decreased during the duration of the biofilm growth in all of the treatments. In summary, the biofilms were discrete at the beginning of the cultivation period. Along with the biofilm growth, the discrete microalgae fragments combined and became an integrated biofilm resulting in the decrease of the biofilm porosity (Tang et al., 2016).

As shown in Fig. 4c, bubbles due to the settlement of microalgae

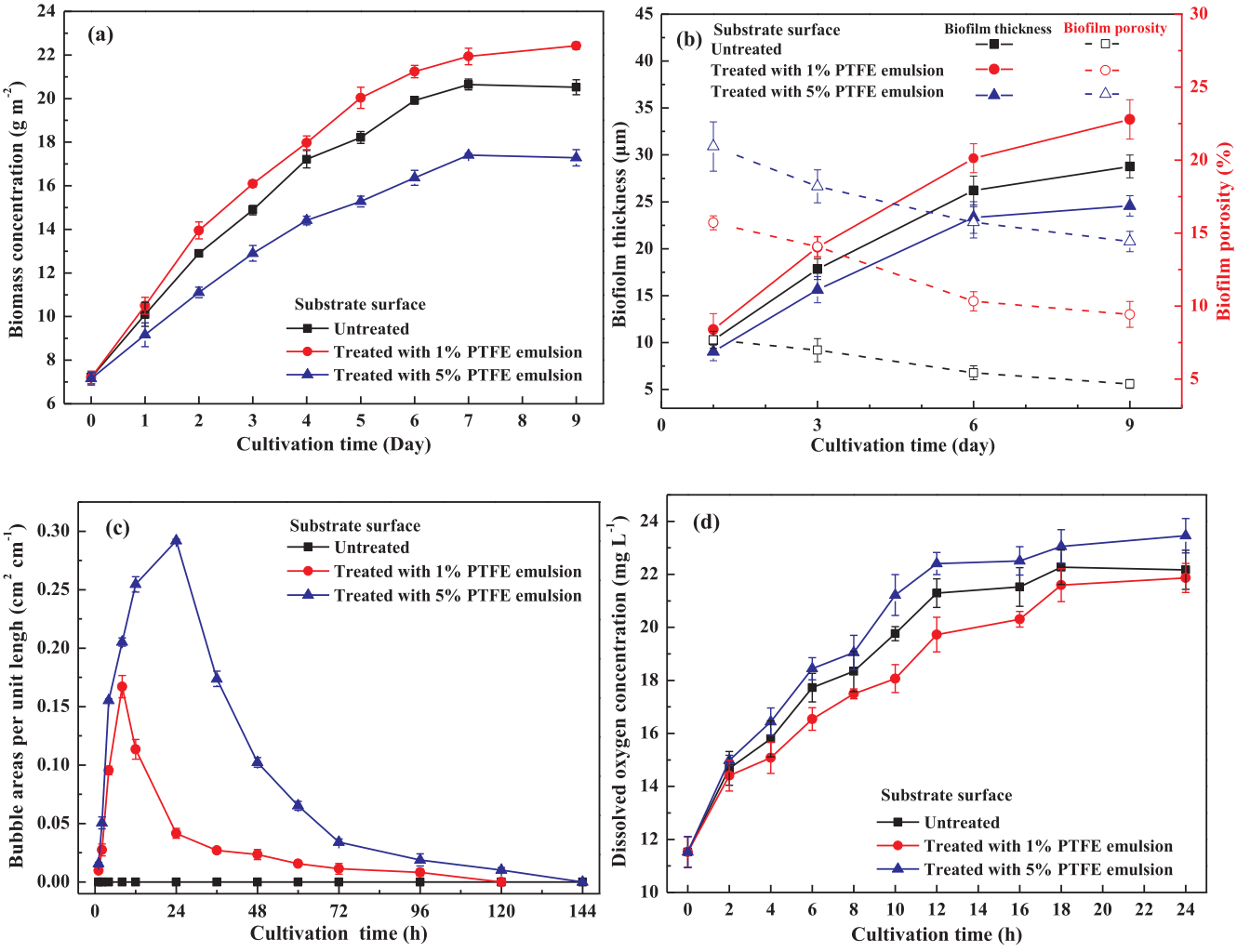

Fig. 4. Biomass concentration (a), biofilm thickness and porosity (b), adhered bubble changing curves (c) and dissolved oxygen concentration (d) of *S. obliquus* biofilms on different substrate surfaces.

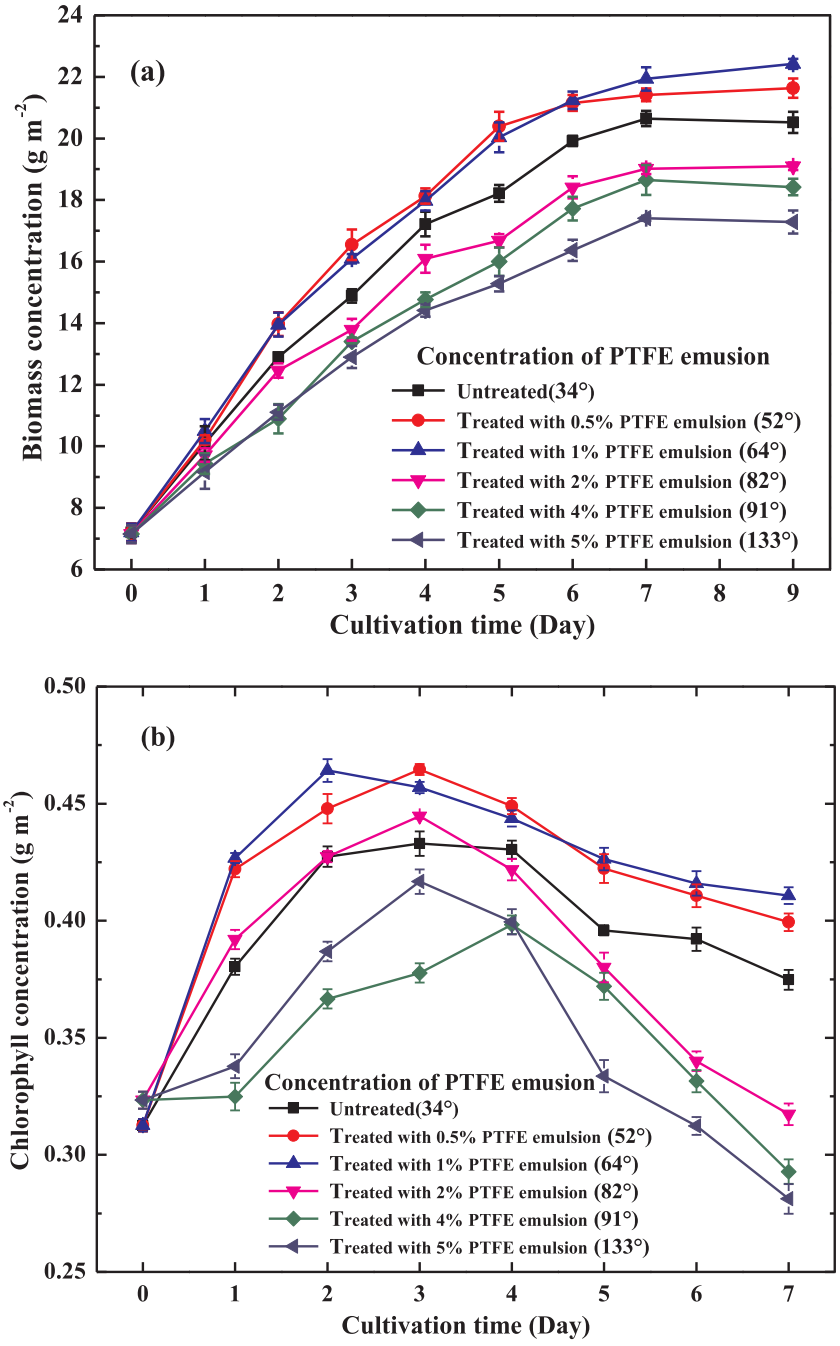

Fig. 5. Effects of treated concentration of PTFE emulsion on *S. obliquus* biofilm biomass concentrations (a) and chlorophyll concentrations (b).

were among the largest changes over the previous 24 h. In addition, the bubble area per unit length sharply increased to maximum values (0 $cm^2\ cm^{-1}$, 0.11 $cm^2\ cm^{-1}$, and 0.29 $cm^2\ cm^{-1}$ with the substrate surfaces of untreated, treated with 1% PTFE emulsion, treated with 5% PTFE emulsion, respectively). Therefore, the biofilm on the treated surfaces was looser and more porous than those on the untreated surfaces due to the effects of bubble behavior (Fig. 4b). Due to the adhered bubbles that occupied the surfaces, some biofilm sites became little holes at the initial attachment period. Along with the bubble detachment and the biofilm growth, these holes made the biofilm a porous microcosm. However, when bubbles detached from the substrate surface and rose in the liquid, they not only carried off the microalgae cells around them but also disturbed the liquid in the medium. Thus, a small portion of the microalgae cells were brought back into the liquid medium, and most of the cells settled down on the substrate surface due to gravity. These cycled processes help the biofilm form a porous microstructure so that light, nutrients and carbon source could transfer effectively in the porous biofilm (Guimerà et al., 2016). On the other hand, the microalgae cells were divorced from the biofilm and backed to the medium. So these cells rolled over in the cultivation medium and fully absorbed nutrients, which could lead to a higher cellular activity and greater growth potential. Once these cells settled again, the biofilm growth condition would be optimized.

While microalgae formed a biofilm during the first 12 h, the cells released a large amount of oxygen that adhered to the substrate surface. At this period, bubble behaviors were mainly affected by the substrate properties and the growth of the microalgae. Furthermore, the maximum value of the bubble area per unit length increased as the contact angle of the substrate surface increased. This result agrees with that of a previous study (Byakova et al., 2003). After reaching the maximum value, the bubble area per unit length began to decrease very quickly during the 12th and 48th hours. This phenomenon could be due to the

fast growth of the microalgae biofilm. The discrete microalgae biofilms combined with one another and became an integrated biofilm, which weakened the impact of substrate properties on the bubble behavior. As the microalgae grew, the biofilm biomass gradually covered the substrate surface. The dominant factor affecting bubble behavior changed into the growth of microalgae biofilm. It was notable that there was still a small change in the bubble area per unit length from 48 h to 72 h. This effect may be attributed to the fact that bubble behaviors still proceeded at the sites during the initial sedimentation period. After this period, biofilm biomass totally covered the substrate surface, and the bubbles dissolved and disappeared completely. Thereafter, bubble behaviors no longer affect the biofilm growth.

Furthermore, bubble behaviors (detachment and rising) could disturb the medium liquid and contribute to the diffusion of dissolved oxygen, so that the DO on the upper layer of the substrate surface treated with 1% PTFE emulsion was lower than that in the other treatments (Fig. 4d). Oxygen is the metabolic product during the photosynthesis of microalgae cells. In fact, if oxygen build-up occurs (i.e., when the concentration of dissolved oxygen in the culture is above its counterpart in equilibrium with its partial pressure in the atmosphere), the reversible reaction of photosynthesis is shifted to the left, thus decreasing photosynthetic efficiency; in general, oxygen concentrations above air saturation inhibit photosynthesis in microalgae. Besides, accumulation of O_2 in the liquid culture medium is one of the most difficult problems to overcome, because it may become toxic above a certain threshold; dissolved oxygen concentrations above 35 mg/L, which are toxic to most microalgae (Carvalho et al., 2006). Thus, DO diffusion could avoided the accumulation of metabolic products and minimized the possibility of product inhibition of the reactions, which were beneficial for the microalgae growth. Therefore, too many adhered bubbles resulted in excessive amounts of DO around the biofilm. For example, the DO upper layer of the substrate surface treated with 5% PTFE emulsion. The higher concentration of DO caused the product inhibition of the reactions, which were harm for the microalgae growth. Obviously, bubble adhesion was beneficial for biofilm growth within limits.

These results demonstrated that the change in the substrate surface properties by the spraying of PTFE had a complicated effect on microalgae biofilm formation and growth. Thus, further investigation for this impact was necessary.

3.3. Effects of substrate surface treatment using different concentration of PTFE emulsion on S. obliquus biofilm growth

According to the results of the previous sections of this study, microalgae biofilms were affected by the behaviors of adhered bubbles. However, the beneficial range of bubble behaviors for biofilm growth was not clear. Thus, to evaluate the optimal treated concentration of PTFE emulsion treated on substrate surfaces, six levels of substrates were prepared to tests their effects on biofilm growth.

Fig. 5 shows biomass concentrations and chlorophyll concentrations on the substrate surfaces with different wettabilities. Collectively, Fig. 5a demonstrates that the substrates treated with the 1% PTFE emulsion offered the best surface characteristics for microalgae biofilm growth, with a yield of approximately 22.42 g m^{-2} and a productivity of 2.49 g m^{-2} day^{-1}. The following biomass concentration yields were, in order, 21.63 g m^{-2} with the sprayed concentration of 0.5%, a contact angle of 52°, 20.52 g m^{-2} with the untreated surfeces, a contact angle of 34°, 19.09 g m^{-2} with the sprayed concentration of 2%, a contact angle of 82°, 18.42 g m^{-2} with the sprayed concentration of 4%, a contact angle of 91°, and 17.28 g m^{-2} with the sprayed concentration of 5%, a contact angle of 133°. Thus, it is safe to conclude that bubble adhesion to the treated substrate surface leads to a porous biofilm microstructure compared to the biofilm on the untreated substrate. This porous microstructure was able to minimize transfer resistance and improve the mass transfer efficiency between the biofilm and the surrounding environment. As a result, the biofilm biomass on some treatment substrates (sprayed concentration of 0.5% and 1%) accumulated more effectively than that on the untreated substrate surface. However, an excess of adhered bubbles had a negative influence on biofilm growth. As mentioned above, bubble adhered increased with the increasing of surface wettablities and roughness. Excessive bubbles were harmful to the nutrients and carbon source transfer and resulted in poor biomass accumulation. In addition, large pores made the biofilm too loose and easily detached. Furthermore, adhered bubbles partially limited the growth space of the biofilm. Thus, the biofilm biomass concentrations tended to decrease when the sprayed concentration of PTFE emulsion on the substrate surfaces increased from 2% to 5%. Notably, the biomass concentration on the surface with 1% PTFE treated was beyond that on the surface with 0.5% PTFE treated at the 6th day. The reason for this phenomenon may be that adhered than on the 52° surface and negatively impacted biofilm growth during the early growth period. Later, the bubbles gradually dissolved and detached from the substrate surface (Fig. 4c). The higher porous microstructure of 1% PTFE treated surface provided a large advantage for biofilm growth.

As the main light-harvesting molecule for photosynthetic organisms, there is an approximately linear relationship between chlorophyll concentration and light conversion efficiency (Delgadovargas et al., 2000). Fig. 5b showed the tendency of chlorophyll concentration to change over time. At approximately the first 4 days, the chlorophyll concentration increased rapidly. This result implied that the microalgae cells were more active and that the biomass accumulated effectively in a manner similar to the growth pattern observed in Fig. 5a. The microalgae cells in this experiment obtained their carbon source from the air, which limited their degree of photosynthesis. Therefore, the chlorophyll concentrations tended to decrease at the later growth period.

From the perspective of economics, the market price of PTFE (HESEN, Shanghai) used in this study is about $26 a kilogram. The optimizing concentration of PTFE emulsion in this study was 1%. And quantity for spray on the substrate surfaces was 0.0125 L m^{-2}. Thus, the induced cost of this treatment was about $0.325 a square meter. And the commercial price of microalgae biomass is around $13 per kilogram. In this case, the incremental gains of biomass obtained from the treated surface per square meter is $2.2, which is much higher than $0.325 per square meter of the treatment cost. Furthermore, the treated substrate can be reused more than ten times for microalgae biofilm growth. Therefore, the introduced cost is much lower.

4. Conclusions

Bubble adhesion and detachment occurred only on the PTFE-treated surfaces that were hydrophobic and rough. These bubble behaviors made the biofilm more porous with attendant benefits for CO_2 and nutrient transfer. Therefore, the biofilm biomass production increased by 9.26–22.42 g m^{-2} on the 1% PTFE-treated surface. Conversely, bubble detachment stirred up microalgae cells in the biofilm and decreased its concentration by 15.30% on the 5% PTFE-treated surface. Therefore, to optimize microalgae biofilm cultivation, further study should be conducted to balance the benefits of the bubbles with the problems they create.

Acknowledgements

The authors gratefully acknowledge the financial support from the National Key Research and Development Program – China (No. 2016YFB0601002), the International Cooperation and Exchanges NSFC – China (No. 51561145013), and the National Science Foundation for Young Scientists – China (No. 51606020).

References

Attard, P., 2003. Nanobubbles and the hydrophobic attraction. Adv. Colloid. Interfac. 104, 75–91.

Bachmann, J., Horton, R., Ploeg, R.R.V.D., Woche, S., 2000. Modified sessile drop method for assessing initial soil-water contact angle of sandy soil. Soil. Sci. Soc. Am. J. 64 (2), 564–567.

Berner, F., Heimann, K., Sheehan, M., 2015. Microalgal biofilms for biomass production. J. Appl. Phycol. 27 (5), 1793–1804.

Byakova, A.V., Gnyloskurenko, S.V., Nakamura, T., Raychenko, O.I., 2003. Influence of wetting conditions on bubble formation at orifice in an inviscid liquid: mechanism of bubble evolution. Colloid Surf. A. 229 (1), 19–32.

Chang, H., Huang, Y., Fu, Q., Liao, Q., Zhu, X., 2016. Kinetic characteristics and modeling of microalgae *Chlorella vulgaris* growth and CO_2 biofixation considering the coupled effects of light intensity and dissolved inorganic carbon. Bioresour. Technol. 206, 231–238.

Chang, H., Fu, Q., Huang, Y., Xia, A., Liao, Q., Zhu, X., 2017. Improvement of microalgae lipid productivity and quality in an ion-exchange-membrane photobioreactor using real municipal wastewater. Int. J. Agr. Biol. Eng. 10 (1), 97.

Carvalho, A.P., Meireles, L.A., Malcata, F.X., 2006. Microalgal reactors: a review of enclosed system designs and performances. Biotechnol. Progr. 22 (6), 1490–1506.

Chisti, Y., 2007. Biodiesel from microalgae. Biotechnol. Adv. 25 (3), 294–306.

Christenson, L.B., Sims, R.C., 2012. Rotating algal biofilm reactor and spool harvester for wastewater treatment with biofuels by-products. Biotechnol. Bioeng. 109 (7), 1674–1684.

Delgadovargas, F., Jiménez, A.R., Paredeslópez, O., 2000. Natural pigments: carotenoids, anthocyanins, and betalains – characteristics, biosynthesis, processing, and stability. Crit. Rev. Food. Sci. 40 (3), 173–289.

Ditscherlein, L., Fritzschea, J., Peuker, U.A., 2016. Study of nanobubbles on hydrophilic and hydrophobic alumina surfaces. Colloid Surf. A. 497, 242–250.

Gião, M.S., Montenegro, M.I., Vieira, M.J., 2005. The influence of hydrogen bubble formation on the removal of *Pseudomonas fluorescens* biofilms from platinum electrode surfaces. Process. Biochem. 40 (5), 1815–1821.

Gross, M., Mascarenhas, V., Wen, Z., 2015. Evaluating algal growth performance and water use efficiency of pilot-scale revolving algal biofilm (RAB) culture systems. Biotechnol. Bioeng. 112 (10), 2040.

Guimerà, X., Dorado, A.D., Bonsfills, A., Gabriel, G., Gabriel, D., Gamisans, X., 2016. Dynamic characterization of external and internal mass transport in heterotrophic biofilms from microsensors measurements. Water. Res. 102, 551.

Huang, Y., Xiong, W., Liao, Q., Fu, Q., Xia, A., Zhu, X., Sun, Y., 2016. Comparison of *Chlorella vulgaris* biomass productivity cultivated in biofilm and suspension from the aspect of light transmission and microalgae affinity to carbon dioxide. Bioresour. Technol. 222, 367–373.

Huang, Y., Zhao, S., Ding, Y.D., Liao, Q., Huang, Y., Zhu, X., 2017. Optimizing the gas distributor based on CO_2 bubble dynamic behaviors to improve microalgal biomass production in an air-lift photo-bioreactor. Bioresour. Technol. 233, 84–91.

Liao, Q., Zhu, X., Zheng, X., Ding, Y., 2007. Visualization study on the dynamics of CO_2 bubbles in anode channels and performance of a DMFC. J. Power. Sources 171, 644–651.

Liu, C., Xiao, T.M., Jing, Z., Lei, Z., Yang, J.L., Ming, Z., 2014. Effect of membrane wettability on membrane fouling and chemical durability of SPG membranes used in a microbubble-aerated biofilm reactor. Sep. Purif. Technol. 127, 157–164.

Lorenzen, C.J., 1967. Determination of chlorophyll and pheopigments: spectrophotometric equations. Limnol. Oceanogr. 12 (2), 343–346.

Ozkan, A., Kinney, K., Katz, L., Berberoglu, H., 2012. Reduction of water and energy requirement of algae cultivation using an algae biofilm photobioreactor. Bioresour. Technol. 114, 542–548.

Pereira, M.M., Kurnia, K.A., Sousa, F.L., Silva, N.J., Lopesdasilva, J.A., Coutinho, J.A., Freire, M.G., 2015. Contact angles and wettability of ionic liquids on polar and non-polar surfaces. Phys. Chem. Chem. Phys. 17 (47), 31653.

Qu, X., Liao, Q., Zhu, X., Gao, X., Wang, Y., Tian, X., 2011. Visual experiment of interaction between photosynthetic bacteria and gas-liquid interface in microspace. CIESC. J. 62 (1), 163–169.

Rios, P.F., Dodiuk, H., Kenig, S., McCarthy, S., Dotan, A., 2007. The effect of polymer surface on the wetting and adhesion of liquid systems. J. Adhes. Sci. Technol. 21 (3–4), 227–241.

Schnurr, P.J., Allen, D.G., 2015. Factors affecting algae biofilm growth and lipid production: a review. Renew. Sust. Energ. Rev. 52, 418–429.

Schnurr, P.J., Espie, G.S., Allen, D.G., 2014. The effect of light direction and suspended cell concentrations on algal biofilm growth rates. Appl. Microbiol. Biotechnol. 98 (20), 8553–8562.

Shen, Y., Yuan, W., Pei, Z.J., Wu, Q., Mao, E., 2009. Microalgae mass production methods. T. Asabe. 52 (4), 1275–1287.

Shen, Y., Zhu, W., Chen, C., Nie, Y., Lin, X., 2016. Biofilm formation in attached microalgal reactors. Bioproc. Biosyst. Eng. 39 (8), 1281–1288.

Stephens, E., Ross, I., King, Z., Mussgnug, J.H., Kruse, O., Posten, C., Borowitzka, M.A., Hankamer, B., 2010. An economic and technical evaluation of microalgal biofuels. Nat. Biotechnol. 28 (2), 126–128.

Sun, Y., Liao, Q., Huang, Y., Xia, A., Fu, Q., Zhu, X., Zheng, Y., 2016. Integrating planar waveguides doped with light scattering nanoparticles into a flat-plate photobioreactor to improve light distribution and microalgae growth. Bioresour. Technol. 220, 215–224.

Surman, S.B., Walker, J.T., Goddard, D.T., Morton, L.H.G., Keevil, C.W., Weaver, W., Skinner, A., Hanson, K., Caldwell, D., Kurtz, J., 1996. Comparison of microscope techniques for the examination of biofilms. J. Microbiol. Meth. 25 (1), 57–70.

Tang, B., Yu, C., Bin, L., Zhao, Y., Feng, X., Huang, S., Fu, F., Ding, J., Chen, C., Li, P., 2016. Essential factors of an integrated moving bed biofilm reactor-membrane bioreactor: adhesion characteristics and microbial community of the biofilm. Bioresour. Technol. 211, 574–583.

Tang, H.P., Zhu, J.L., Xi, Z.P., Di, X.B., Wang, J.Y., Ao, Q.B., 2010. Impact factors of fractal analysis of porous structure. Sci. China. Technol. Sci. 53 (2), 348–351.

Tsolcha, O.N., Tekerlekopoulou, A.G., Akratos, C.S., Bellou, S., Aggelis, G., Katsiapi, M., Moustaka-Gouni, M., Vayenas, D.V., 2015. Treatment of second cheese whey effluents using a Choricystis-based system with simultaneous lipid production. J. Chem. Technol. Biot. 91 (8), 2349–2359.

Wang, J., Wei, W., 2009. Factors influencing fermentative hydrogen production: a review. Int. J. Hydrogen. Energ. 34 (2), 799–811.

Yang, W., Li, J., Ye, D., Zhu, X., Liao, Q., 2017. Bamboo charcoal as a cost-effective catalyst for an air-cathode of microbial fuel cells. Electrochimi. Acta. 224, 585–592.

Zhang, X., Liu, B., Wang, J., Zhang, Z., Shi, K., Wu, S., 2014. Adobe photoshop quantification (PSQ) rather than point-counting: a rapid and precise method for quantifying rock textural data and porosities. Comput. Geosci-UK 69, 62–71.

Zheng, H.R., Wang, X.W., Lin, X.H., Geng, Q., Chen, X., Dai, W.X., Wang, X.X., 2012. Promoted effect of polyethylene glycol on the photo-induced hydrophilicity of TiO_2 films. Acta. Phys-Chim. Sin. 28 (7) 1764-1770(7).

Zheng, Y., Huang, Y., Liao, Q., Zhu, X., Fu, Q., Xia, A., 2016. Effects of wettability on the growth of *Scenedesmus obliquus* biofilm attached on glass surface coated with polytetrafluoroethylene emulsion. Int. J. Hydrogen. Energ. 41 (46), 21728–21735.